JTE
HCMUTE
ISSN: 2615-9740

JOURNAL OF TECHNICAL EDUCATION SCIENCE
Ho Chi Minh City University of Technology and Education
Website: https://jte.edu.vn
Email: jte@hcmute.edu.vn

Upper Bound Limit Analysis of 2D Structures Using Lagrange Extraction-Based Isogeometric Analysis

Van Hien Do
Ho Chi Minh City University of Technology and Education, Vietnam

*Corresponding author. *Email: hiendv@hcmute.edu.vn*

ARTICLE INFO

Received: 05/04/2023
Revised: 14/05/2023
Accepted: 23/05/2023
Published: 28/10/2023

KEYWORDS

Limit analysis;
Isogeometric analysis;
SOCP;
Upper bound method;
Lagrange extraction.

ABSTRACT

This work presents a new approach that uses Lagrange extraction-based isogeometric analysis and Second Order Cone Programming (SOCP) to determine the limit load factor in two-dimensional problems. This methodology makes use of an upper-bound limit approach and a rigid-perfectly plastic material model. Lagrange extraction is used to link a C^0 nodal basis to a smooth B-spline basis. This enables the use of straightforward methods for isogeometric analysis in conventional finite element systems. A SOCP problem is created from the limit analysis problem, which may then be solved using Mosek optimization software. The numerical results indicate the correctness and effectiveness of the current technique by contrasting it with other approaches mentioned in the literature.

Doi: https://doi.org/10.54644/jte.79.2023.1372

1. Introduction

Nowadays, the most essential factors in the evaluation of many engineering structures are intended to avoid failure modes, have reliable safety, and be reasonably priced. Limit analysis of the structures, particularly in the chemical industry, nuclear power plants, civil engineering, and metal forming, plays an important role in the design of engineering structures in order to achieve these goals. In structural analysis, one of the most important factors is the collapse limit load factor. Early in the 20th century, the idea of limit analysis is created. The limit load factor can be calculated using either the analytical approach or the numerical method. Gaydon and McCrum [**Error! Reference source not found.**] present the first piece of work utilizing analytic methods for limit analysis. However, due to the complicated problems with applied loads as well as geometry, there are limitations to the theoretical answer in actual engineering. In order to address the general issue in the field of limit analysis, the limit analysis study being conducted today is developing numerical techniques. Numerous computational techniques, including the Finite Element Method (FEM) [**Error! Reference source not found.**,**Error! Reference source not found.**,**Error! Reference source not found.**,**Error! Reference source not found.**,**Error! Reference source not found.**], Meshfree or meshless **Error! Reference source not found.**, **Error! Reference source not found.**], Boundary Element Method (BEM) [**Error! Reference source not found.**], and most recently, IsoGeometric Analysis (IGA) [**Error! Reference source not found.**, **Error! Reference source not found.**,**Error! Reference source not found.**,**Error! Reference source not found.**,**Error! Reference source not found.**,**Error! Reference source not found.**], are presented in the literature for limit analysis. Although the FEM for limit analysis is frequently used in real-world engineering, its mesh creation process is one of its drawbacks. In the analysis of overall time, the mesh generation procedure accounts for 80%. Hughes *et al.* [**Error! Reference source not found.**] recently developed the IGA, which incorporates Finite Element Analysis (FEA) into computer-aided geometric design (CAGD), to address the issue with the computational expense of the FEM structure generation. In contrast to the FEM's Lagrange interpolation, the IGA approach uses Non-Uniform Rational Basis Spline (NURBS) interpolation. The NURBS function has various advantages compared to the Lagrange interpolation function, including a greater continuity of derivatives and the simplicity of increasing the

NURBS function's order without altering the geometry. Due of major discrepancies between the NURBS basis function and the Lagrange function, the computational aspects of the NURBS function pose the question of how to successfully employ the NURBS function in existing FEM methods. Bézier extraction was the first attempt to address this issue. Borden *et al.* [**Error! Reference source not found.**] explored this extraction based on NURBS basis functions in terms of C^0 Bernstein polynomials. Dominik Schillinger and colleagues [**Error! Reference source not found.**] recently introduced Lagrange extraction, which is similar to Bézier extraction but establishes a direct connection between NURBS and Lagrange polynomial basis functions rather than using C^0 Bernstein polynomials as a new shape function in Bézier extraction. In this research, a formulation of Lagrange extraction-based isogeometric analysis combined with SOCP is studied for upper bound limit analysis of two-dimensional structures. The IGA solution can be improved using refinements. The efficiency and convergence of the method for limit analysis of two-dimensional structures are checked through several examples.

The following describes how the paper is organized: The NURBS based on Lagrange extraction and the Lagrange extraction method for limit analysis of structures are briefly discussed in Section 2. Several examples of the suggested approach are provided in Section 3. We conclude our article by making a few final remarks.

2. Upper bound limit analysis using Lagrange extraction-based isogeometric finite element approach

2.1. Lagrange extraction-based isogeometric analysis

The B-spline basis functions are constructed following Ref [**Error! Reference source not found.**] based on a given knot vector $\Xi = \{\xi_1, \xi_2, \ldots, \xi_{n+p+1}\}$ as

For $p = 0$

$$N_{i,0}(\xi) = \begin{cases} 1 & \xi_i \le \xi < \xi_{i+1} \\ 0 & \text{otherwise} \end{cases} \tag{1}$$

For $p \ge 1$

$$N_{i,p}(\xi) = \frac{\xi - \xi_i}{\xi_{i+p} - \xi} N_{i,p-1}(\xi) + \frac{\xi_{i+p+1} - \xi}{\xi_{i+p+1} - \xi_{i+p}} N_{i+1,p-1}(\xi). \tag{2}$$

The definition of the B-spline curve is

$$C(\xi) = \sum_{i=1}^{n} N_{i,p}(\xi) \boldsymbol{P}_i = \boldsymbol{P}^T \boldsymbol{N}(\xi) \tag{3}$$

The B-spline function based on the element can be expressed in a different format as

$$N_{a,p}^e(\xi) = \sum_{b=1}^{p+1} \alpha_{ab} L_{b,p}(\xi) \ \ or \ \boldsymbol{N}^e(\xi) = \boldsymbol{D}^e \boldsymbol{L}(\xi) \tag{4}$$

When Eq. (4) is substituted into Eq. (3), Eq. (3) for the segment of the B-spline curve in Figure 1 may be expressed as

$$C^e(\xi) = (\boldsymbol{P}^e)^T \boldsymbol{N}^e(\xi) = (\boldsymbol{P}^e)^T \boldsymbol{D}^e \boldsymbol{L}(\xi) = (\boldsymbol{P}^{l,e})^T \boldsymbol{L}(\xi) \tag{5}$$

Where $\boldsymbol{L}(\xi), \boldsymbol{D}^e$ and $\boldsymbol{P}^{l,e}$ are a basis Lagrange basis function, Operator for the Lagrange extraction of the element *e* and nodal points of Lagrange for element *e*, respectively.

In one dimensional space, the entire Lagrange extraction operator may be written as

$$\boldsymbol{D}^e = \begin{bmatrix} N_{1,p}^e(\hat{\xi}_1) & N_{1,p}^e(\hat{\xi}_2) & \cdots & N_{1,p}^e(\hat{\xi}_{p+1}) \\ N_{2,p}^e(\hat{\xi}_1) & N_{2,p}^e(\hat{\xi}_2) & \cdots & N_{2,p}^e(\hat{\xi}_{p+1}) \\ \vdots & \vdots & \cdots & \vdots \\ N_{p+1,p}^e(\hat{\xi}_1) & N_{p+1,p}^e(\hat{\xi}_2) & \cdots & N_{p+1,p}^e(\hat{\xi}_{p+1}) \end{bmatrix} \tag{6}$$

The NURBS basis function on each element can be defined in matrix form as

$$\boldsymbol{R}^e(\xi) = \frac{1}{W(\xi)} \boldsymbol{W} \boldsymbol{N}^e(\xi) \tag{7}$$

Where $W(\xi)$ and $\boldsymbol{W}$ are the weight function and the diagonal matrix of weights, respectively. These functions are defined as

$$W(\xi) = \sum_{b=1}^{p+1} w_b N_{b,p}^{e}(\xi) = \boldsymbol{w}^T \boldsymbol{N}(\xi) \tag{8}$$

where

$$\boldsymbol{W} = \begin{bmatrix} w_1 & & & \\ & w_2 & & \\ & & \ddots & \\ & & & w_{p+1} \end{bmatrix}$$

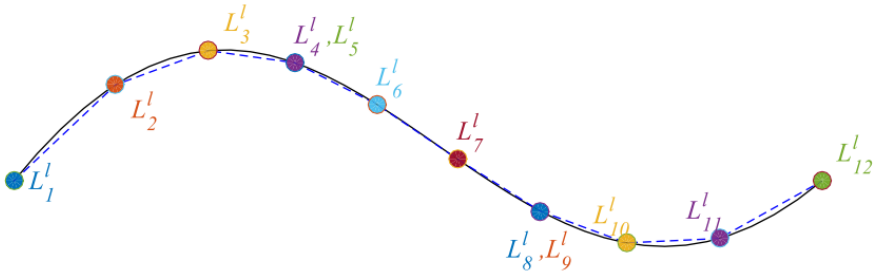

Figure 1. *Nodal Lagrange points and the B-spline curve*

One way to express the NURBS curve is as

$$C(\xi) = \boldsymbol{P}^T \boldsymbol{R}(\xi) = \frac{1}{W(\xi)} \boldsymbol{P}^T \boldsymbol{W} \boldsymbol{N}^e(\xi) \tag{9}$$

In terms of the nodal Lagrange basis functions, NURBS curve can be obtained by substitution Eq. (4) into Eq. (9)

$$C(\xi) = \boldsymbol{P}^T \boldsymbol{R}(\xi) = \frac{1}{W(\xi)} \boldsymbol{P}^T \boldsymbol{W} \boldsymbol{D} \boldsymbol{L}(\xi) = \frac{1}{W(\xi)} (\boldsymbol{D}^T \boldsymbol{W} \boldsymbol{P})^T \boldsymbol{L}(\xi) \tag{10}$$

Eq. (8) is expressed as follows using the nodal Lagrange basis functions:

$$W(\xi) = \boldsymbol{w}^T \boldsymbol{N}(\xi) = \boldsymbol{w}^T \boldsymbol{D} \boldsymbol{L}(\xi) = (\boldsymbol{D}^T \boldsymbol{w})^T \boldsymbol{L}(\xi) = (\boldsymbol{w}^l)^T \boldsymbol{L}(\xi) \tag{11}$$

The Lagrange control points may be computed as

$$\boldsymbol{P}^L = (\boldsymbol{W}^l)^{-1} \boldsymbol{D}^T \boldsymbol{W} \boldsymbol{P} \tag{12}$$

In terms of nodal Lagrange basis functions, the NURBS curve can be expressed as

$$C(\xi) = \boldsymbol{P}^T \boldsymbol{R}(\xi) = \frac{1}{W(\xi)} \boldsymbol{P}^T \boldsymbol{W} \boldsymbol{N}^e(\xi) = \frac{1}{W(\xi)} (\boldsymbol{D}^T \boldsymbol{W} \boldsymbol{P})^T \boldsymbol{L}(\xi) = \sum_{a=1}^{n} \frac{w_a^l L_{a,p}(\xi)}{W^l(\xi)} \boldsymbol{P}^L \tag{13}$$

In summary, a set of C^o nodal Lagrange curves can represent the NURBS curve.

2.2. Kinematic formulation and solution procedure of the discrete problem

A rigid, perfectly plastic body is considered with boundary $\Gamma = \Gamma_t \cup \Gamma_u$ and $\Gamma_t \cap \Gamma_u = \emptyset$, where Γ_t is the static boundary and Γ_u is the kinematic boundary. The constrained boundary Γ_u is fixed. Body forces f and surface tractions g on Γ_t are applied to the body. According to the kinematic theorem, By solving the following mathematical programming, the upper bound load multiplier λ^+ can be found as

$$\lambda^+ = \min D(\dot{\varepsilon}) \tag{14}$$

where strain rates $\dot{\varepsilon}$ is given by

$$\dot{\varepsilon} = [\dot{\varepsilon}_{xx} \quad \dot{\varepsilon}_{yy} \quad \dot{\varepsilon}_{xy}] = \sum_e \boldsymbol{B}_e \dot{\boldsymbol{u}}_e \tag{15}$$

$\boldsymbol{B}_e$ is the strain matrix and is expressed as

$$\boldsymbol{B}_e = \begin{bmatrix} \dfrac{\partial \boldsymbol{R}_e}{\partial x} & 0 & \dfrac{\partial \boldsymbol{R}_e}{\partial y} \\ 0 & \dfrac{\partial \boldsymbol{R}_e}{\partial y} & \dfrac{\partial \boldsymbol{R}_e}{\partial x} \end{bmatrix}^T \tag{16}$$

The plastic dissipation $D(\dot{\varepsilon})$ is given by

$$D(\dot{\varepsilon}) = \underbrace{\max}_{\psi(\sigma)\leq 0} \sigma : \dot{\varepsilon} \equiv \sigma_\varepsilon : \dot{\varepsilon} \tag{17}$$

where σ represents the admissible stresses contained inside the convex yield surface $\psi(\sigma)$ and σ_ε denotes the yield surface stresses associated with any strain rates ε due to the plasticity condition. Plastic dissipation may be quantified using strain rates

$$\mathrm{D}(\dot{\varepsilon}) = \int_\Omega \sigma_0 \sqrt{\dot{\varepsilon}^T \Theta \dot{\varepsilon}}\, d\Omega = \sum_{e=1}^{nel} \int_{\Omega^e} \sigma_0 \sqrt{\dot{\varepsilon}^{eT} \Theta \dot{\varepsilon}^e}\, d\Omega^e \tag{18}$$

where

$$\Theta = \frac{1}{3}\begin{bmatrix} 4 & 2 & 0 \\ 2 & 4 & 0 \\ 0 & 0 & 1 \end{bmatrix} \tag{19}$$

$\dot{\varepsilon}^e$ is plastic strains rate of element e and σ_0 is the yield stress. Eq. (18) computed at Gauss points over each element e becomes as follows:

$$D(\dot{\varepsilon}) = \sum_{e=1}^{nel} \sum_{i=1}^{eGP} \sigma_0 \bar{w}_i |J_i| \sqrt{\dot{\varepsilon}_i^T \Theta \dot{\varepsilon}_i} = \sum_{i=1}^{nGP} \sigma_0 \bar{w}_i |J_i| \sqrt{\dot{\varepsilon}_i^T \Theta \dot{\varepsilon}_i} \tag{20}$$

The Eq. (20) may be stated in the form of a sum of norms as

$$D(\dot{\varepsilon}) = \sum_{i=1}^{nGP} \sigma_0 \bar{w}_i |J_i| \left\| \boldsymbol{C}_f^T \dot{\boldsymbol{\varepsilon}}_i \right\| = \sum_{i=1}^{nGP} \sigma_0 \bar{w}_i |J_i| \, \|\boldsymbol{\rho}_i\| \tag{21}$$

where $\bar{w}_i$, $|J_i|$ and $\dot{\varepsilon}_i$ are the weight value, a Jacobian matrix determinant and plastic strains rate at the Gauss point i, respectively. $nGP = nel \times eGP$ is the total number of the Gauss points of problem. $\|\,.\,\|$ in the plastic dissipation function is the Euclidean norm, $\|\mathrm{v}\| = \sqrt{(\mathrm{v}^T \mathrm{v})}$ and The Cholesky factor of Θ is represented by $\boldsymbol{C}_f$ in Eq. (22)

$$\boldsymbol{C}_f = \frac{1}{\sqrt{3}}\begin{bmatrix} 2 & 0 & 0 \\ 1 & \sqrt{3} & 0 \\ 0 & 0 & 1 \end{bmatrix} \tag{22}$$

and $\boldsymbol{\rho}_i = [\rho_1 \quad \rho_2 \quad \rho_3]^T = \boldsymbol{C}_f^T \dot{\boldsymbol{\varepsilon}}_i$ is a vector of additional variables to make the optimization problem in Eq. (14) into a sum of norm problem as

$$\lambda^+ = \min \sigma_0 \sum_{i=1}^{nGP} \bar{w}_i |J_i| \|\boldsymbol{\rho}_i\|$$

subjected to:

$$\begin{cases} \dot{\boldsymbol{u}} = 0 \qquad on\ \Gamma_u \\ \boldsymbol{\rho}_i = \boldsymbol{C}_f^T \dot{\boldsymbol{\varepsilon}}_i \\ \dot{\boldsymbol{\varepsilon}}_i = \sum_{i=1}^{nGP} \boldsymbol{B}_i^e \dot{\boldsymbol{u}}_e \\ W_{ex}(\dot{\boldsymbol{u}}) = 1 \end{cases} \tag{23}$$

JTE
HCMUTE
ISSN: 2615-9740

JOURNAL OF TECHNICAL EDUCATION SCIENCE
Ho Chi Minh City University of Technology and Education
Website: https://jte.edu.vn
Email: jte@hcmute.edu.vn

In order to efficiently solve the limit analysis problem, the Mosek optimization package is used in the research. By introducing the new variables $\boldsymbol{t_i}$, the problem in Eq. (23) becomes as follows

$$\lambda^+ = \min \sigma_0 \sum_{i=1}^{nGP} \overline{w}_i |J_i| t_i$$

subjected to:

$$\begin{cases} \dot{\boldsymbol{u}} = 0 & on\ \Gamma_u \\ \|\boldsymbol{\rho}_i\| \le t_i & \forall i = 1{:}\, nGP \\ \boldsymbol{\rho}_i = \boldsymbol{C}_f^T \dot{\boldsymbol{\varepsilon}}_i \\ \dot{\boldsymbol{\varepsilon}}_i = \sum_{i=1}^{nGP} \boldsymbol{B}_i^e \dot{\boldsymbol{u}}_e \\ W_{ex}(\dot{\boldsymbol{u}}) = 1 \end{cases} \quad (24)$$

where the second constraint in Eq. (24) represents quadratic cones.

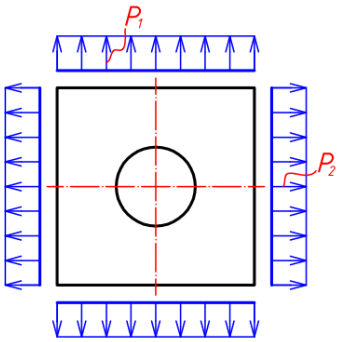

Figure 2. *Full model with two loads.*

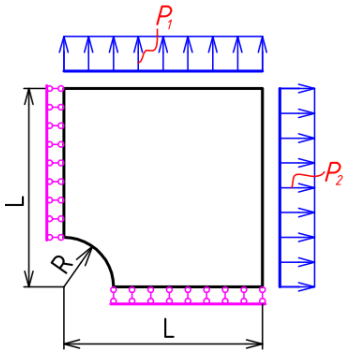

Figure 3. *Symmetric model with two loads and boundary conditions*

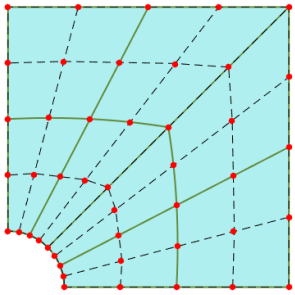

Figure 4. *16 elements of Quadratic NURBS mesh and control points.*

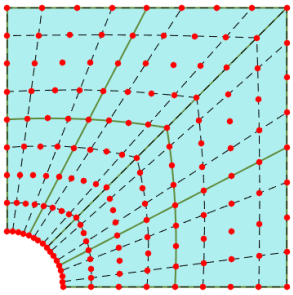

Figure 5. *Quartic of NURBS mesh and control points.*

3. Numerical validations

Through a number of benchmark problems in this section, we evaluate the effectiveness of the new method. A few instances are used to validate the methodology with analytical and literature-based solutions.

Table 1. *The square plate with a central circular hole's limit load factor under the current approach*.

Load cases	Polynomial order	Mesh discretization		
		2(2 × 2)	2(4 × 4)	2(8 × 8)
$P_2 = 0$	2nd degree	0.8160	0.8089	0.8038
	3rd degree	0.8143	0.8083	0.8032
	4th degree	0.8103	0.8076	0.8043

$P_2 = P_1/2$	2nd degree	0.9237	0.9169	0.9133
	3rd degree	0.9205	0.9151	0.9124
	4th degree	0.9174	0.9152	0.9128
$P_2 = P_1$	2nd degree	0.9047	0.8987	0.8966
	3rd degree	0.8995	0.8971	0.8961
	4th degree	0.8978	0.8964	0.8958

3.1. Square plate with a central circular hole

In the first illustration, two distinct load cases, P_1 and P_2, are applied to a square plate with a central circular hole. Figure 2 depicts the complete model for this issue. The upper-right quarter of the plate with length L, height L, and radius $R/L = 0.2$ is modelled due to the symmetry of the applied weight and geometry. $L = 2$ boundary conditions are then applied, as seen in Figure 3. Numerous researchers [**Error! Reference source not found.**, **Error! Reference source not found.**,**Error! Reference source not found.**, **Error! Reference source not found.**, **Error! Reference source not found.**, **Error! Reference source not found.**] have investigated this issue. The plane stress condition and the von Mises elastic-plastic material model are adopted in our investigation. The following material properties are selected: Yield stress σ_y = 116.2 MPa, Young's modulus E = 2.1e^5 MPa, and Poisson's ratio v = 0.3.

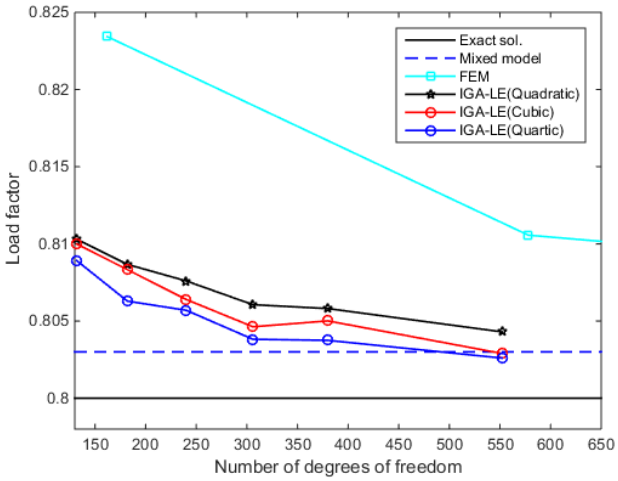

Figure 6. *The convergence of the current approach in comparison to other solutions for $P_2 = 0$.*

In this research, the mesh is discretized using a multi-patch of NURBS elements with 2nd , 3rd and 4th degrees polynominal, respectively, using 128 NURBS elements with 380 degree of freedom (DOF), 98 NURBS elements with 380 DOF, and 72 NURBS elements with 380 DOF. Figure 7 shows an illustration of an IGA model.

Table 2. *Comparison of various numerical methods for limit analysis.*

Authors	**Methods**	**Loading cases**		
		$P_2 = P_1$	$P_2 = P_1/2$	$P_2 = 0$
Belytschko [**Error! Reference source not found.**]	Equilibrium FE (LB)	---	---	0.780
Gross-Weege [**Error! Reference source not found.**]	Reduced basis technique (LB)	0.882	0.891	0.782
Zhang *et al.* [**Error! Reference source not found.**]	BEM (LB)	0.893	0.907	0.789
Nguyen & Palgen **Error!**	Equilibrium FE (LB)	0.704	---	0.564

Reference source not found.]				
Chen *et al.* [**Error! Reference source not found.**]	EFG (LB)	0.874	0.899	0.798
Zouain *et al.* [**Error! Reference source not found.**]	mixed model	0.894	0.911	0.803
Gaydon *et al.* [**Error! Reference source not found.**]	Analytical	---	---	0.8
Present (ISO-LE)	Quartic	0.8966	0.9133	0.8038
	Cubic	0.8961	0.9129	0.8050
	Quadratic	0.8960	0.9134	0.8058

Table 1 contains a list of the results from this case. The current solution is compared to other ones that are presented in the literature in Table 2. Table 2 shows how well our answer agrees with the other solutions, including FEM [**Error! Reference source not found.**], BEM [**Error! Reference source not found.**], EFG **Error! Reference source not found.**, **Error! Reference source not found.**], and others [**Error! Reference source not found.**, **Error! Reference source not found.**]. The convergence of the current method in comparison to other methods is shown in Fig. 5. It is reasonable to conclude that our results quickly converge to the exact solution.

3.2. A symmetric continuous beam

The second problem is a symmetric continuous beam subjected to two uniform separate loads P_1 and P_2, as shown in Figure 7. Young's modulus E = 1.8x10^5 MPa, Poisson's ratio v = 0.3, and Yield stress σ_y = 100 MPa are the material's properties.

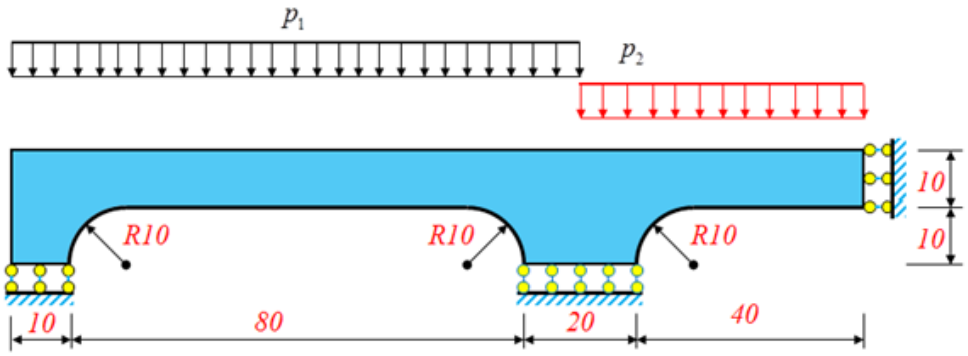

Figure 7. *Geometry, loads and boundary conditions of the symmetric continuous beam*

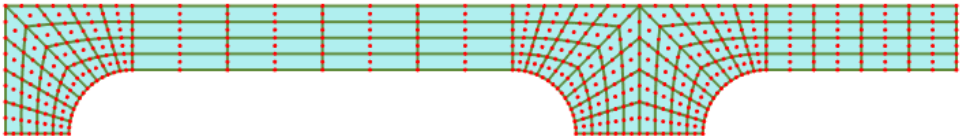

Figure 8. *NURBS mesh and control points for the symmetric continous beam*.

Figure 8 provides a description of the discretization of isogeometric finite element using 128 quadratic NURBS elements. Table 3 lists the limit values. The obtained solutions are in good agreement with the results reported in Refs [**Error! Reference source not found.**,**Error! Reference source not found.**,**Error! Reference source not found.**,**Error! Reference source not found.**].

Table 3. *Comparison of various numerical methods for limit analysis.*

Authors	Methods	Loading cases (MPa)			
		$p_1 = 2$ $p_2 = 0$	$p_1 = 0$ $p_2 = 1$	$p_1 = 1{,}2$ $p_2 = 1$	$p_1 = 2$ $p_2 = 1$
Garcea *et al.* [**Error! Reference source not found.**]	Numerical	3.280	8.718	5.467	3.280
Ho *et al.* [**Error! Reference source not found.**]	Equilibrium ES-FEM	3.301	8.748	5.504	3.302
Nguyen *et al.* [**Error! Reference source not found.**]	NS-FEM-T3	3.297	8.722	5.493	3.296
Do *et al.*[**Error! Reference source not found.**]	Quadratic - dual algorithm	3.322	8.781	5.538	3.322
	Cubic - dual algorithm	3.305	8.744	5.508	3.305
	Quartic - dual algorithm	3.295	8.723	5.493	3.295
Nguyen *et al.* [**Error! Reference source not found.**]	ES-FEM-T3	3.402	9.192	5.720	3.386
Present (ISO-LE)	Quadratic	3.375	8.845	5.568	3.375
	Cubic	3.392	8.811	5.643	3.392

4. Conclusions

The upper bound limit load factor of 2D structure problems is computed using a novel numerical method in this paper that combines the SOCP and NURBS-based Lagrange extraction. Numerical examples are given to show how the current approach is accurate and efficient in comparison to other technique solutions. The following conclusions are drawn from the number tests:

- The current method demonstrated some benefits of the IGA in terms of refinement flexibility, precise geometry, and connection of the smooth spline basis to the C^0 Lagrange polynomials basis, which led to more accurate solutions than those provided by other methods.
- The findings of this investigation show close agreement with the analytical solutions and other available ones.

Future 3D structure problems will be addressed using the present methodology.

REFERENCES

[1] F. A. Gaydon and A. W. McCrum, "A theoretical investigation of the yield point loading of a square plate with a central circular hole," *Journal of Mechanics and Physics Solids*, vol. 2, pp. 156-169, 1951, doi: 10.1016/0022-5096(54)90022-8.

[2] R. Casciaro and L. Cascini, "A mixed formulation and mixed finite elements for limit analysis," *International Journal for Numerical Methods in Engineering*, vol. 18, pp. 211-243, 1982, doi: 10.1002/nme.1620180206.

[3] T. Belytschko, "Plane stress shakedown analysis by finite elements," *International Journal of Mechanic Sciences*, vol. 14, pp. 619–625, 1972, doi: 10.1016/0020-7403(72)90061-6.

[4] J. G. Weege, "On the numerical assessment of the safety factor of elasto-plastic structures under variable loading," *International Journal of Mechanics and Sciences*, vol. 39, pp. 417–433, 1997, doi: 10.1016/S0020-7403(96)00039-2.

[5] G. Garcea, G. Armentano, S. Petrolo, and R. Casciaro, "Finite element shakedown analysis of two-dimensional structures," *International Journal for Numerical Methods in Engineering*, vol. 63, pp. 1174–1202, 2005, doi: 10.1002/nme.1316.

[6] A. Makrodimopoulos and C. M. Martin, "Upper bound limit analysis using simplex strain elements and second-order cone programming," *Int. J. Numer. Anal. Meth. Geomech.*, vol. 31, pp. 835-865, 2007, doi: https://doi.org/10.1002/nag.567.

[7] J. S. Chen, C. T. Wu, S. Yoon, and Y. You, "A stabilized conforming nodal integration for Galerkin mesh-free methods," *International Journal for Numerical Methods in Engineering*, vol. 50, pp. 435–466, 2001, doi: 10.1002/1097-0207(20010120)50:2.

[8] S. Chen, Y. Liu, and Z. Cen, "Lower-bound limit analysis by using the EFG method and non-linear programming," *International Journal for Numerical Methods in Engineering*, vol. 74, pp. 391–4157, 2008, doi: 10.1002/nme.2177.

[9] Z. Zhang, Y. Liu, and Z. Cen, "Boundary element methods for lower bound limit and shakedown analysis," *Engineering Analysis with Boundary Elements*, vol. 28, pp. 905–917, 2004, doi: 10.1016/S0955-7997(03)00117-6.

[10] H. V. Do and H. N. Xuan, "Limit and shakedown isogeometric analysis of structures based on Bézier extraction," *European Journal Mechanics and Solid*, vol. 63, pp. 149–164, 2017, doi: 10.1016/j.euromechsol.2017.01.004.
[11] H. V. Do and H. N. Xuan, "Computation of limit and shakedown loads for pressure vessel components using isogeometric analysis based on Lagrange extraction," *International Journal of Pressure Vessels and Piping*, vol. 169, pp. 57–70, 2019, doi: 10.1016/j.ijpvp.2018.11.012.
[12] V. Gupta *et al*., "An Insight on NURBS Based Isogeometric Analysis, Its Current Status and Involvement in Mechanical Applications," *Arch. Computat. Methods Eng.*, vol. 30, pp. 1187–1230, 2023, doi: https://doi.org/10.1007/s11831-022-09838-0.
[13] X. Wei, D. Liu, and S. Yin, "An Isogeometric Bézier Finite Element Method for Vibration Optimization of Functionally Graded Plate with Local Refinement," *Crystals*, vol. 12, no. 6, p. 830, 2022, doi: https://doi.org/10.3390/cryst12060830.
[14] V. H. Do, "Application of isogeometric analysis to free vibration of truss structures," *Journal of Technical Education Science*, no. 42, pp. 20–27, 2021. [Online]. Available: https://jte.edu.vn/index.php/jte/article/view/373.
[15] D. V. Hien, H. N. Bon, and V. H. Thinh, "Limit analysis for plane stress problem by using nurbs based on bézier extraction in combination with second order cone program," *Journal of Technical Education Science*, no. 52, pp. 17–24, 2019. [Online]. Available: https://jte.edu.vn/index.php/jte/article/view/200.
[16] T. J. R. Hughes, J. A. Cottrell, and Y. Bazilevs, "Isogeometric analysis: CAD, finite elements, NURBS, exact geometry and mesh refinement," *Computer Methods in Applied Mechanics and Engineering*, vol. 194, pp. 4135–4195, 2005, doi: 10.1016/j.cma.2004.10.008.
[17] M. J. Borden, M. A. Scott, J. A. Evans, and T. J. R. Hughes, "Isogeometric finite element data structures based on Bézier extraction of NURBS," *International Journal for Numerical Methods in Engineering*, vol. 86, pp. 15 – 47, 2011, doi: 10.1002/nme.2968.
[18] D. Schillinger, P. K. Ruthal, and L. H. Nguyen, "Lagrange extraction and projection for NURBS basis functions: a direct link between isogeometric and standard nodal finite element formulations," *International Journal for Numerical Methods in Engineering*, vol. 108, pp. 515–534, 2016, doi: 10.1002/nme.5216.
[19] Z. Zouain, L. Borges, and J. L. Silveira, "An algorithm for shakedown analysis with nonlinear yield functions," *Computer Methods in Applied Mechanics and Engineering*, vol. 191, pp. 2463–2481, 2002, doi: 10.1016/S0045-7825(01)00374-7.
[20] F. A. Gaydon and A. W. McCrum, "A theoretical investigation of the yield point loading of a square plate with a central circular hole," *Journal of Mechanics and Physics Solids*, vol. 2, pp. 156-169, 1951, doi: 10.1016/0022-5096(54)90022-8.
[21] P. L. H. Ho, C. V. Le, and T. Q. Chu, "The equilibrium cell-based smooth finite element method for shakedown analysis of structures," *International Journal Computational Methods*, vol. 16, no. 6, p. 1840013, 2017, doi: 10.1142/S0219876218400133.
[22] H. N. Xuan, T. Rabczuk, T. N. Thoi, T. N. Tran, and N. N. Thanh, "Computation of limit and shakedown loads using a node-based smoothed finite element method," *International Journal for Numerical Methods in Engineering*, vol. 90, pp. 287–310, 2012, doi: 10.1002/nme.3317.
[23] D. H. Nguyen and L. Palgen, "Shakedown analysis by displacement method and equilibrium finite elements," in *Proceedings of SMIRT-5*, Berlin, German, 1979, doi: 10.1139/tcsme-1980-0006.

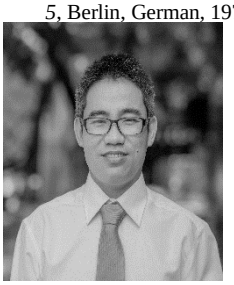

Do Van Hien (M'83) received the B.S. degree in engineering mechanics in 2005, the M.S. degree in mechanical engineering in 2012 and PhD in engineering mechanics in 2020 from HCMC University of Technology and Education, Ho Chi Minh City, Viet Nam. His research interests include computional mechanics and numerical methods. From 2007 to 2009, he was a research and development engineer at UMC Akasaka Technical Center, Okayama, Japan. His research interest includes the development of gasket and bearing seal for automobile. From 2017 to 2018, he was a guest researcher at Computational Mechanics, Bauhaus Weimar University, Germany. From 2009 until now, he worked as Lecturer at the Faculty of Mechanical Engineering, HCMUTE Email address: hiendv@hcmute.edu.vn